Desalination and Water Treatment
www.deswater.com

doi:10.5004/dwt.2018.22387

127 (2018) 334–342
September

Fenton oxidation of Diamine Blue 3B using heterogeneous catalyst based on hydroxyapatite nanoparticles

Atena Dehghanpour Farashah[a], Saeedeh Hashemian[a,*], Fatemeh Tamaddon[b]

[a]*Department of Chemistry, Yazd Branch, Islamic Azad University, Yazd, Iran, Tel. +983187572; Fax: +983538214810; emails: sa_hashemian@iauyazd.ac.ir (S. Hashemian), atenafarashahi@yahoo.com (A.D. Farashah)*
[b]*Department of Chemistry, Yazd University, Yazd 89195-741, Iran, email: ftamaddon@yazd.ac.ir*

Received 13 February 2017; Accepted 13 April 2018

ABSTRACT

In this study, degradation of Diamine Blue 3B (DB) azo dye by Fenton oxidation process (Fe^{2+}/H_2O_2) was investigated. Hydroxyapatite (HAP) was used as heterogeneous catalyst for oxidation of DB. HAP was synthesized and characterized by Fourier transform infrared spectroscopy, scanning electron microscopy, transmission electron microscopy and X-ray diffraction methods. The optimal conditions for the degradation of DB were determined at pH = 6.0, HAP = 500 mg L^{-1}, Fe^{2+} = 9.8 × 10^{-3} mg L^{-1} and H_2O_2 = 100 mg L^{-1}. The results of experiments showed that degradation of DB dye could be described with a pseudo-second-order kinetic model. The results of thermodynamic implied that the oxidation process was feasible, spontaneous and endothermic. The HAP was conveniently regenerated after four cycles.

Keywords: Fenton's reagent; Hydroxyapatite; Heterogeneous catalysis; Diamine Blue 3B; Oxidation

1. Introduction

Azo dyes are used in large quantities in several industries such as textile, cosmetic, paper, drug and food processing. They are known as the largest group of synthetic colorants and difficult to degrade by biological treatment methods due to their complex structure and their stability [1]. Most of dyes are carcinogenic, harmful and reduces the light diffusion in aqueous systems; thus causing a negative effect on photosynthesis and are harmful to human health. A massive amount of azo dyes from these sources is discharged into natural waterways. Azo dyes constituting 60%–70% of all dyes produced are extensively used in textile industry due to their chemical stability and versatility [2].

Therefore, decolorization and detoxicity of dye effluents have received increasing attention. Biological methods by living organisms or fungi are ineffective to degrade dyes if the large, chemical refractory and stable molecule of aromatics compounds present in dyes, so treatment cannot be based on biodegradation alone. The complete removal of pollutant from wastewater is therefore necessary and subject to widespread research. Several processes have been studied to reach partial or complete degradation of pollutant compounds such as adsorption, coagulation, biodegradation and chemical or photochemical degradation [3–7]. Physical methods such as adsorption are technically easy and low cost process but non-destructive, that is, they just transfer the pollutants from aqueous solution to another phase rather than destroy them. Various adsorbents such as activated carbon [8], sepiolite [9], vermiculite [10] and carbon nanotube [11,12] were used to remove dyes from aqueous solution. Activated carbon is the most widely used adsorbent to remove pollutants from water [6,13–17]. On the other hand, physical processes are expensive operations [18]. Advanced oxidation processes (AOPs) are becoming more important technologies for wastewater treatment. Essentially, there are three main types of AOPs depending on the type of oxidant (oxygen, ozone, and hydrogen peroxide). The wastewater treatment by AOP with oxygen and ozone is very expensive and usually acts under high temperatures (200°C–325°C) and pressure (50–150 bar). AOP based on H_2O_2 is considered to be one of the most effective, simple and economical methods that can oxidize and

* Corresponding author.

degrade many organic compounds and synthetic dyes. AOPs are based on the generation of very reactive species such hydroxyl radical ($^{\bullet}OH$) that oxidize a broad range of pollutants quickly and non-selectively [19–21]. Fenton process as an important AOP technology has been attracting growing interest. In classic Fenton chemistry, the reaction between hydrogen peroxide and Fe^{2+} in an acidic aqueous solution is generally recognized to produce hydroxyl radicals. In the past few years, many catalysts such as TiO_2, ZnO, WO_3, SnO_2, ZrO_2, CeO_2, CdS and ZnS have been used for photodegradation [22–24]. Catalyzed, uncatalyzed and photocatalyzed decomposition of hydrogen peroxide produces highly reactive species which can degrade a broad range of organic pollutants. The generally accepted free radical chain mechanism for the Fenton reaction is shown as follows [25,26]:

$$Fe^{2+} + H_2O_2 \rightarrow Fe^{3+} + {}^{\bullet}OH + OH^- \quad (1)$$

$$^{\bullet}OH + H_2O_2 \rightarrow H_2O + HO_2^{\bullet} \quad (2)$$

$$Fe^{3+} + HO_2^{\bullet} \rightarrow Fe^{2+} + H^+ + O_2 \quad (3)$$

$$Fe^{2+} + HO_2^{\bullet} \rightarrow Fe^{3+} + {}^{-}HO_2 \quad (4)$$

$$Fe^{2+} + {}^{\bullet}OH \rightarrow Fe^{3+} + OH^- \quad (5)$$

$$HO_2^{\bullet} + {}^{\bullet}OH \rightarrow H_2O + O_2 \quad (6)$$

The photocatalytic degradation of DB by nanocomposites is reported in the literature [27,28]. Hydroxyapatite (HAP) is one of the weak alkaline calcium phosphate which is slightly soluble in water. HAP [$(Ca_5(PO_4)_3(OH)$] has received considerable attention due to its ion-exchange ability, adsorption capacity, macroligand behavior and acid–base properties [24]. HAP is widely used as an implant material in clinical applications owing to its biocompatibility. HAP is widely used as catalyst because it has strong adsorption ability, surface acidity or basicity and ion-exchange ability [29–31]. Apart from the clinical applications, HAP has also been used as a novel support for gold ruthenium catalysts and employed in water gas shift reactions [32] and as catalyst for dehalogenation with molecular hydrogen [33]. The use of HAP for photocatalytic degradation of dyes was studied [34–38]. HAP shows photocatalytic behavior for decomposition of methyl mercaptane under UV irradiation [39].

The main objective of this work is to prepare HAP and determine the catalytic activity of HAP for degradation of Diamine Blue 3B (DB) dye by the Fenton process. The effect of different parameters such as amount of HAP, pH of media, concentration of H_2O_2, concentration of Fe^{2+}, initial DB dye concentration and temperature was investigated. The kinetics and thermodynamics of oxidation were also studied.

2. Experimental

2.1. Materials and methods

All of the reagents in the experiments were of analytical grade (Merck) and were used without further purification. All the experiments were conducted at room temperature. DB 3,3′-[(3,3′-dimethyl[1,1′-biphenyl]-4,4′-diyl)bis(azo)]bis [5-amino-4-hydroxy-2,7-naphthalenedisulfonic acid] was used as the contaminant. It is diazo dye and has chemical formula $C_{34}H_{24}N_6O_{14}S_4$ (772.88 g mol^{-1} and λ_{max}/nm = 590). Fig. 1 shows the molecular structure of DB dye.

The stock solution of 500 mg L^{-1} of DB was prepared and working solutions are prepared by dilution. The oxidation of DB dye was achieved by Fenton's reagent (mixture of $FeSO_4 \cdot 7H_2O$ and H_2O_2). The necessary quantities of Fe^{2+} and H_2O_2 were added simultaneously in the dye solution. All experiments were conducted in a 500 mL thermostated batch glass reactor equipped with the magnetic stirrer. All of these studies were done in the absence and the presence of HAP. The kinetics of oxidation was followed by taking samples at regular time interval. The residual concentration of the DB in the solution at different times of sampling was determined. The residual concentration of the dye was deducted from the calibration curves which were produced at wavelength corresponding to the maximum of absorbance (590 nm) on an UV-visible spectrophotometer apparatus (Shimadzu 160 A). The cell used was in quartz 1 cm thickness. The discoloration efficiency of the dye (X) with respect to its initial concentration is calculated as:

$$\% X = ([DB]_0 - [DB]/[DB]_0) \times 100 \quad (7)$$

where $[DB]_0$ and [DB] are the initial and appropriate concentration of DB dye at any reaction time t, respectively.

2.2. Preparation of HAP

Calcium HAP was synthesized by double decomposition according to the procedure described by Rey et al. [40] and Barka et al. [41]. A solution composed of 35.4 g of $Ca(NO_3)_2 \cdot 4H_2O$ (Merck, Germany) in 0.5 L of distilled water was immediately poured at room temperature into a solution composed of 34.8 g of diammonium hydrogen phosphate $(NH_4)_2HPO_4$ in 1 L of distilled water. The pH of the solution was adjusted to seven by ammonia solution. After low agitation for 2 h, the suspension was briefly filtered on a large Büchner funnel, washed with distilled water, dried at 70°C for 48 h and sieved. HAP precipitation was prepared by the following reaction:

$$10Ca(NO_3)_2 + 6(NH_4)_2HPO_4 + 8NH_4OH \rightarrow Ca_{10}(PO_4)_6(OH)_2 + 20NH_4NO_3 + 6H_2O \quad (8)$$

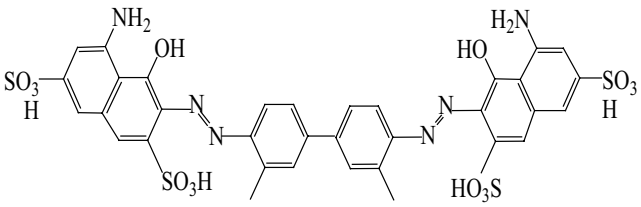

Fig. 1. The molecular structure of DB dye.

3. Results and discussion

3.1. Characterization of HAP

The Fourier transform infrared spectroscopy (FTIR) spectrum of HAP is shown in Fig. 2. The peak at 1,650 cm^{-1} and the broad peak at approximately 3,450 cm^{-1} correspond to the water of crystallization present in the sample. The broadband appeared at around of 1,060, 956 and 562 cm^{-1} are related to different modes of the PO_4^{3-} group in carbonated HAP [31,32]. The ν_1 symmetric stretching mode of phosphate group is observed at 956 cm^{-1}.

Fig. 3 shows the X-ray diffraction (XRD) pattern of HAP. For HAP nanoparticles, the existence of peaks at 2θ approximately 20°, 23.2°, 29.3°, 32.2°, 36° and 40° corresponding to the diffraction planes (100), (211), (210), (300), (102) and (203) of the HAP crystallites, respectively, that confirms the formation and the presence of HAP in products. The hexagonal crystal system P63/m ($a = b = 0.941$, $c = 0.879$) observed for HAP. (These results were confirmed by pattern 86-1199.) The average particles sizes (48–55 nm) of HAP were determined by Deby Sherrer equation.

Fig. 4 shows the scanning electron microscopy (SEM) results of HAP. Fig. 4(a) shows the agglomeration of HAP powders. Energy-dispersive X-ray analysis was also measured to determine the chemical composition of sample. Fig. 4(b) also shows the EDX of HAP. Result from Fig. 4(b) demonstrated that the sample contained only Ca, P and O for HAP. The results of EDX also showed the ratio of Ca/P was 1.67. Transmission electron microscopy (TEM) micrograph of HAP powder was shown in Figs. 5(a) and (b). It was observed the crystal structure of pure HAP vision as rod-like shape with a typical size of 70–100 nm in length and about 50 nm in width.

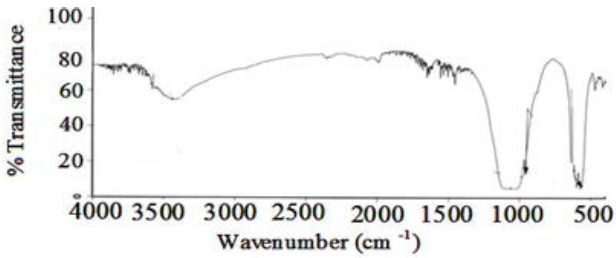

Fig. 2. FTIR spectrum of HAP.

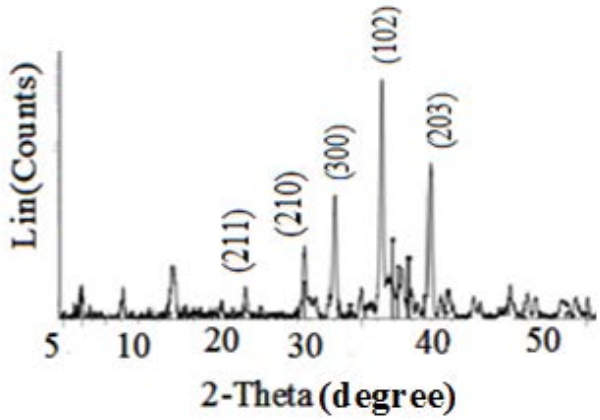

Fig. 3. XRD pattern of HAP.

3.2. Oxidation of DB

The catalytic Fenton oxidation studies were carried out using DB as a probe molecule.

3.2.1. Effect of the amount of H_2O_2

H_2O_2 plays a very important role as a source of •OH generation in the Fenton reaction. The selection of an optimum H_2O_2 concentration for degradation of dyes by Fenton's and photo-Fenton's reagent is important from a practical point of view (due to the cost of H_2O_2). The effect of variation of the amount of H_2O_2 on degradation of DB dye has been investigated in the range from 0.0 to 150 mg L^{-1}. It was discovered that if only Fe^{2+} were added in the solution instead of H_2O_2, DB did not show decomposition. Effect of H_2O_2 dosage on the oxidation of DB is shown in Fig. 6. In the absence of H_2O_2, the rate of oxidation was very slow and the percentage of

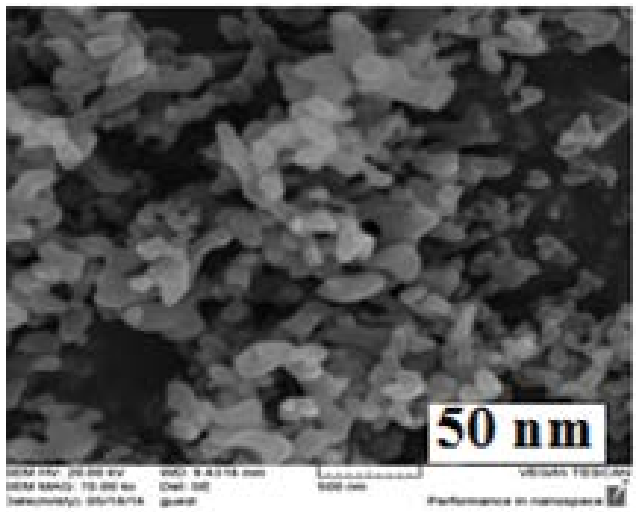

(a)

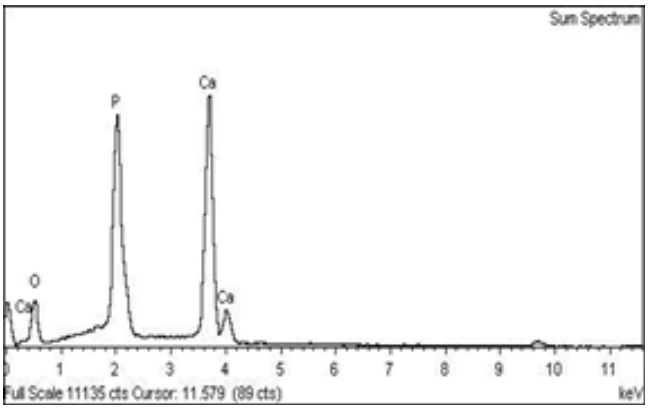

(b)

Fig. 4. (a) SEM micrograph and (b) EDX of HAP nanoparticles.

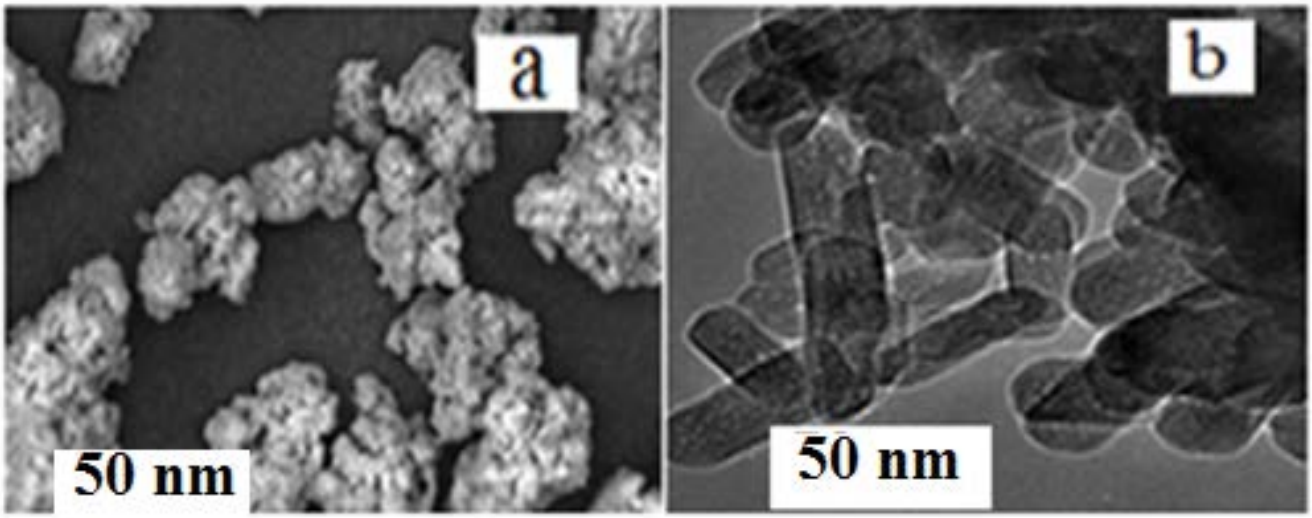

Fig. 5. TEM micrograph of HAP nanoparticles.

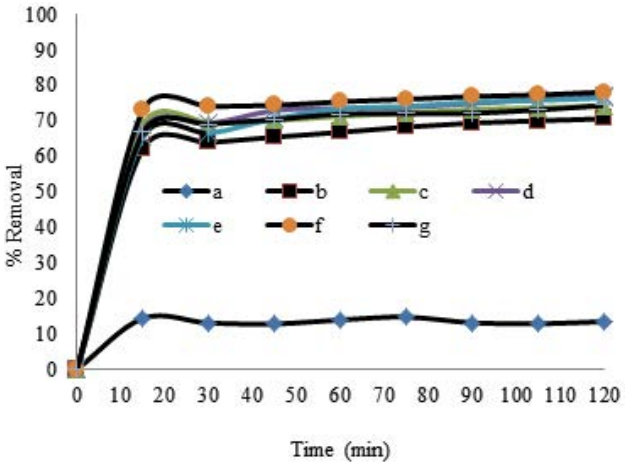

Fig. 6. Effect of H_2O_2 dosage on the catalytic Fenton oxidation of DB (H_2O_2: *a* = 0, *b* = 10, *c* = 20, *d* = 30, *e* = 50, *f* = 100 and *g* = 150 mg L^{-1}) (DB 5 mg L^{-1}, pH 6, Fe^{2+} 5 × 10^{-3} mg L^{-1}, HAP 100 mg L^{-1}, 25°C).

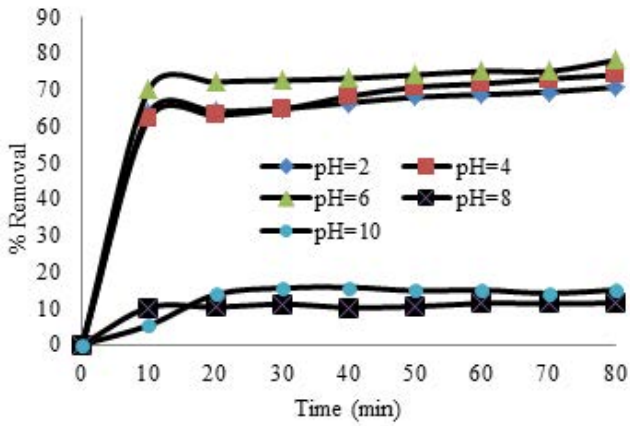

Fig. 7. Effect of pH on DB removal by oxidation Fenton's process in the presence of HAP (DB 5 mg L^{-1}, Fe^{2+} 5 × 10^{-3} mg L^{-1}, H_2O_2 50 mg L^{-1}, HAP 100 mg L^{-1}, 25°C).

oxidation of dye was low. With increasing the concentration of H_2O_2, oxidation of DB dye was increased and H_2O_2 100 mg L^{-1} had the highest DB removal. The increasing concentration of more than 100 mg L^{-1} of H_2O_2 did not cause higher DB removal.

3.2.2. Effect of initial pH

The pH of solution is an important operating parameter affecting on degradation of DB efficiency in AOP. The effect of pH on the degradation of DB has been investigated in pH range 2–10 by adding HCl or NaOH. The effect of initial pH value of solutions on the decolorization of DB by the Fenton oxidation process was shown in Fig. 7. The results indicated that the decolorization of DB was significantly influenced by pH of the solution, and the highest decolorization efficiency was obtained at pH 6.0. The lower efficiency at higher pH values may be due to the precipitation of $Fe(OH)_3$ and therefore, reduces the Fe ions. From Fig. 7, it was observed with an increase in pH range from 2 to 6, the rate of reaction increases and after attaining the maximum value at pH 6.0, the rate decreases with further increase in pH. It affects directly on the mechanism of oxidation of DB dye, because a change in pH of solution involves a variation of the concentration of Fe^{2+}, and therefore the rate of production of OH radicals responsible for oxidation of dyes, will be restricted [42].

3.2.3. Effect of Fe^{2+} dosage

To study the effect of Fe^{2+} dosage on the decolorization of DB by Fenton oxidation, a series of experiments were conducted with different initial concentrations which ranged from 1.4 × 10^{-3} to 9.80 × 10^{-3} mg L^{-1}. The results indicated that the decolorization efficiency of DB increased with increasing the initial concentration of Fe^{2+} in the solution. It can be seen that the decolorization was limited at 1.4 × 10^{-3} mg L^{-1} of Fe^{2+}, and only 65% of DB was degraded within 10 min of reaction.

In the presence of higher values of Fe^{2+}, a great improvement of the decolorization of DB could be observed, and the decolorization efficiency within 10 min of reaction was reached to 98.4%. The fact that higher decolorization efficiency was achieved at high Fe^{2+} dosages was mainly attributable to the higher production of •OH with more Fe^{2+} in the Fenton reaction. The lower degradation capacity of Fe^{2+} at small concentration is probably due to the lowest •OH radicals' production a variable for oxidation [42–44]. Effect of Fe^{2+} dosage on the oxidation of DB is shown in Fig. 8.

3.2.4. Effect of HAP catalyst

The effect of variation of amount of HAP catalyst on the rate of degradation of DB has been studied in the range from 0 to 500 mg. Effect of mass of HAP catalyst on the Fenton oxidation of DB is shown in Fig. 9. An increase in the amount of HAP catalyst to a certain level (500 mg), the rate of degradation increases, which may be regarded as a saturation point.

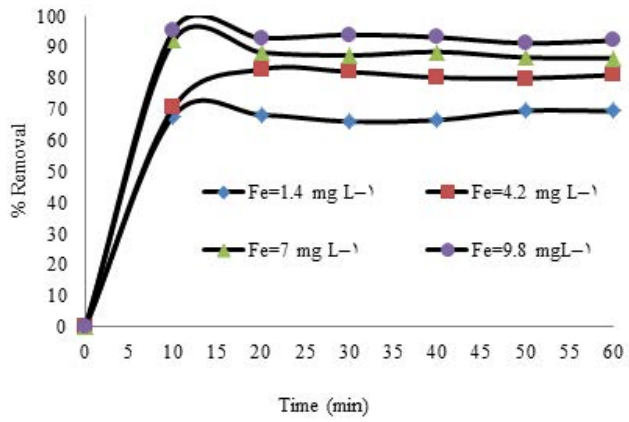

Fig. 8. Effect of Fe^{2+} (mg L^{-1}) dosage (×10^{-3}) on the catalytic Fenton oxidation of DB (DB 5 mg L^{-1}, pH 6, H_2O_2 50 mg L^{-1}, HAP 100 mg L^{-1}, 25°C).

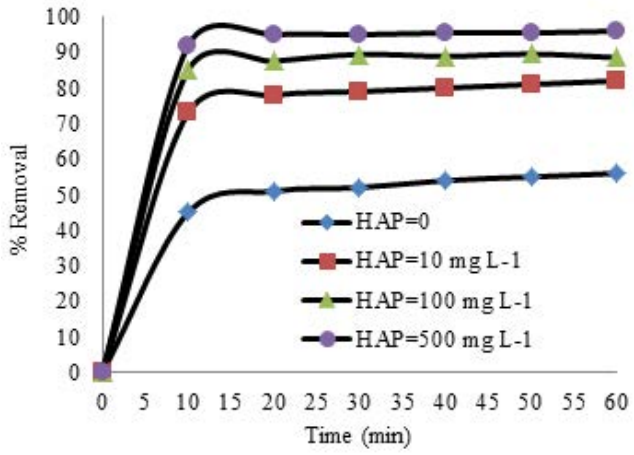

Fig. 9. Effect of HAP amount (mg L^{-1}) on the catalytic Fenton oxidation of DB (DB 5 mg L^{-1}, pH 6, H_2O_2 50 mg L^{-1}, Fe^{2+} 9.8 × 10^{-3} mg L^{-1}, 25°C).

This may be due to an increase in the amount of catalyst; the surface area of catalyst will increase. Additionally, HAP may helps Fe^{2+} ions to attack H_2O_2 and produces hydroxyl radicals, and hence the rate of degradation and oxidation of DB dye also increases. The oxidation process of DB by Fenton oxidation process in the presence of HAP catalyst is shown in Fig. 10.

Fig. 11 also shows the UV-visible absorbance of oxidation of DB at different time interval of A-Fenton oxidation and B-HAP catalytic Fenton oxidation. These results confirmed catalytic effect of HAP for oxidation of DB.

3.2.5. Effect of temperature

The effect of temperature on DB degradation was investigated at 25°C–55°C. It can be seen from Fig. 12 that increasing temperature had a positive effect on the DB degradation. The efficiency of DB removal was increased from 78% to 98.0% when the temperature increased from 25°C to 55°C. Temperature had effect on the reaction between H_2O_2 and Fe^{2+}. This can be explained by the fact that Fenton's reaction could be accelerated by raising the temperature which improved the generation rate of °OH and therefore enhancing the decolorization of DB [45,46].

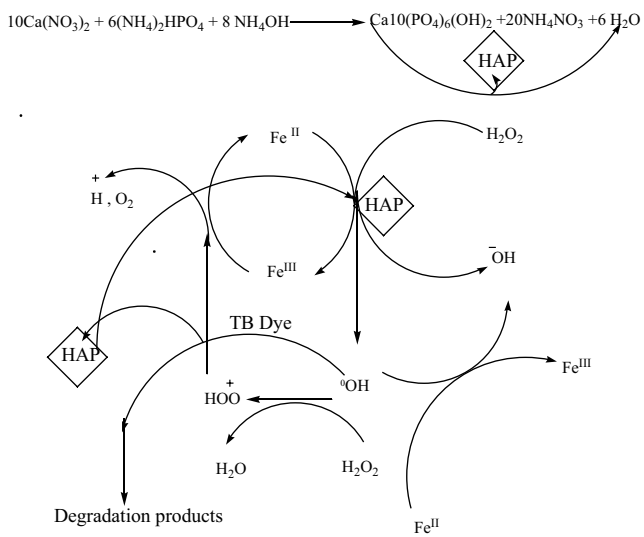

Fig. 10. Fenton oxidation process of DB by HAP catalyst.

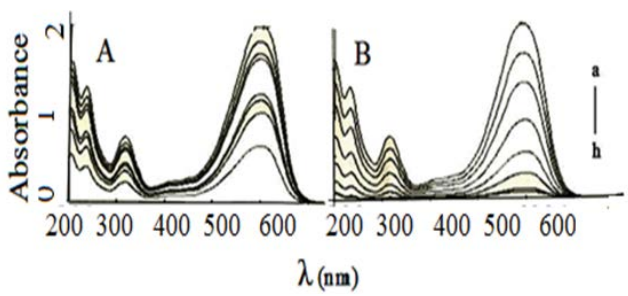

Fig. 11. UV-visible absorption spectra of DB at different time interval of A-Fenton oxidation from 0 to 240 min (*a–h*) and B-HA catalytic Fenton oxidation from 0 to 120 min (*a–h*).

3.2.6. Effect of initial concentration of DB dye

Initial concentration of dye is an important parameter in practical application. The effect of initial DB dye concentrations 4–14 mg L^{-1} on efficiencies of oxidation process was evaluated. As shown in Fig. 13, the degradation of DB efficiency gradually decreased with an increase in the initial concentration. This is due to non-availability of sufficient number of hydroxyl radicals. The presumed reason is that when the initial concentration of DB is increased, the $^{\bullet}OH$ concentration is not increased correspondingly.

3.2.8. Effect of NaCl and Na_2SO_4 salts on Fenton effectiveness

Salts (specifically, sodium chloride and sodium sulfate) are important in using many types of dyes, and they coexist with dyes in the effluent, a fact which could affect the treatment of wastewater [35]. In the presence of inorganic ions, the rate for the reaction of H_2O_2 with ferrous ion is different. Cl^- and SO_4^{2-} are commonly coexisting anions with dyes in wastewater; therefore, the effect of Cl^- and SO_4^{2-} ions on DB removal by Fenton process was investigated. It was found that the presence of NaCl and Na_2SO_4 at the concentration range of 0–100 mg L^{-1} did not have a significant effect on removing DB (Fig. 14).

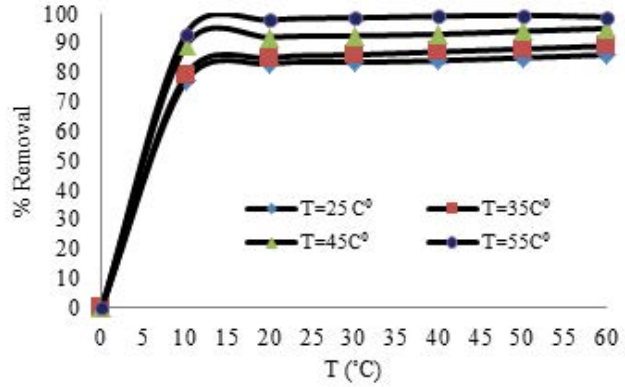

Fig. 12. Effect of temperature (DB 5 mg L^{-1}, 5 pH 6, H_2O_2 50 mg L^{-1}, Fe^{2+} 9.8 × 10^{-3} mg L^{-1}, HAP 500 mg L^{-1}).

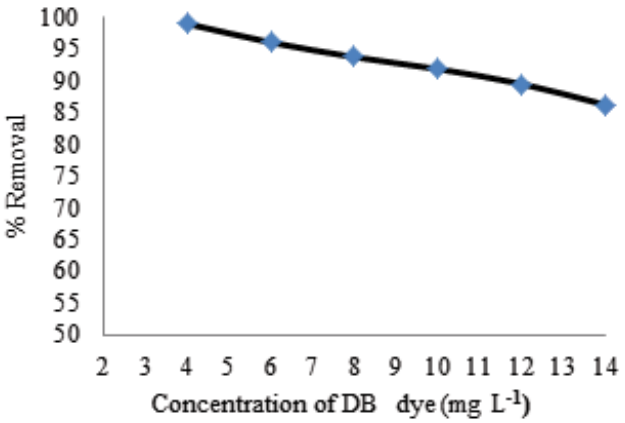

Fig. 13. Effect of concentration of DB dye (mg L^{-1}) (pH 6, H_2O_2 100 mg L^{-1}, Fe^{2+} 9.8 × 10^{-3} mg L^{-1}, HAP 500 mg L^{-1}).

3.3. Kinetic experiments

First-order and second-order kinetic models were used to study the decolorization of DB by the Fenton oxidation process. The individual expression was presented as equations given below: first-order reaction kinetics [46]:

$$-d[C_{(DB)}]/dt = -k_1 C_t \quad (9)$$

Therefore, Eq. (9) was altered to:

$$\ln C_{(DB)}/\ln C_{(DB)_0} = -k_1 t \quad (10)$$

where $C_{(DB)}$ and $C_{(DB)_0}$ are initial concentration of DB and concentration of DB at the any time. A plot of $\ln C_{DB}$ vs. time generated a straight line with a negative slope. The slope of this line corresponds to the apparent rate constant (k_1) value for the degradation of the organic target compound. Rate law of the second-order reaction can be written as follow [47]:

$$1/[C_{(DB)}] - 1/[C_{(DB)_0}] = k_2 t \quad (11)$$

The plot of 1/[C] against t shows the rate constant (k_2) of second-order Fenton reaction. The correlation coefficient value and rate constant for second-order model (R^2 = 0.981 and k_2 = 2.91 × 10^{-1}) are mostly higher than those of the first-order

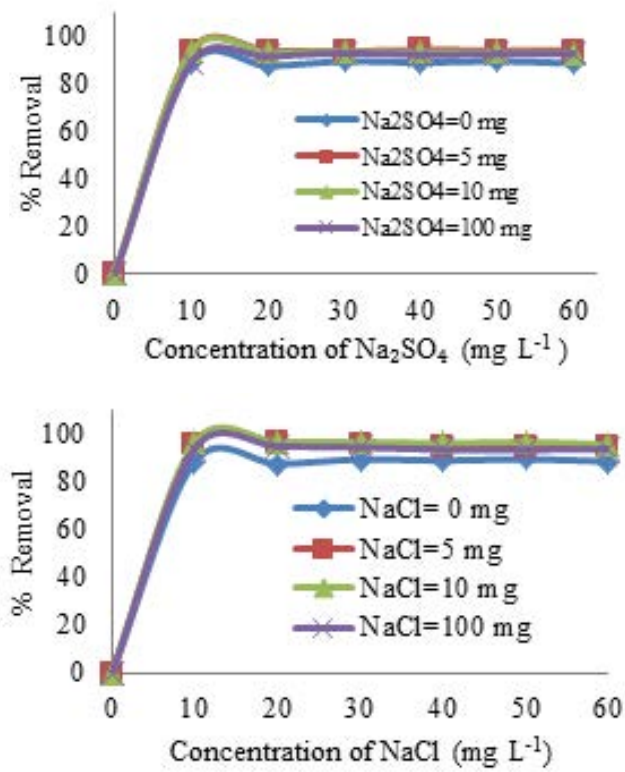

Fig. 14. Effect of NaCl and Na_2SO_4 on Fenton oxidation of DB.

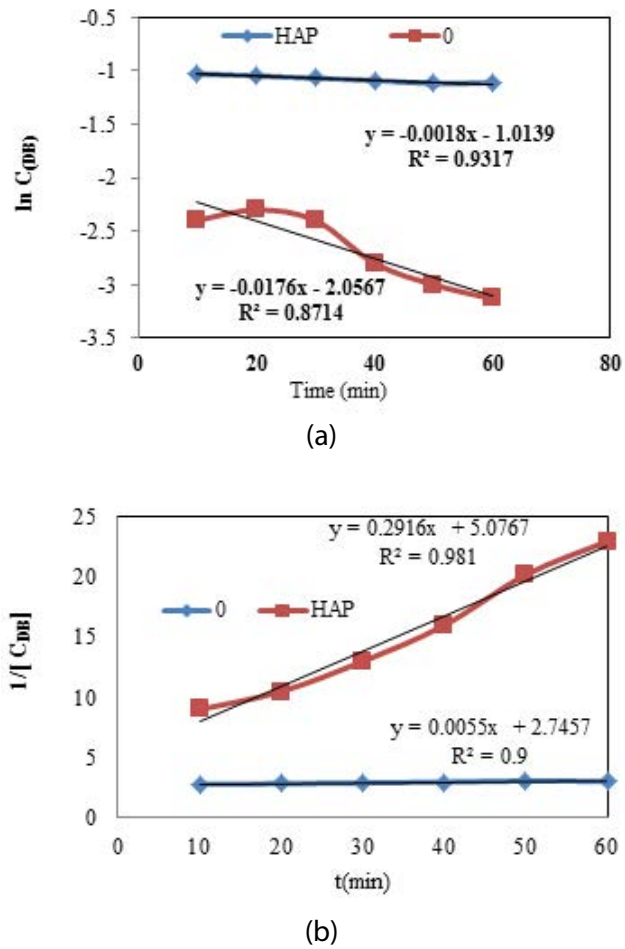

Fig. 15. (a) First-order and (b) second-order reaction kinetics for degradation of DB by Fenton's oxidation (Fe^{2+} 9.8 mg L^{-1}, H_2O_2 100 mg L^{-1} and pH 6.0).

(R^2 = 0.8714 and k_2 = 1.76 × 10^{-2}); therefore, second-order kinetic model is the best model to describe the decolorization of DB by the Fenton's process [47]. Fig. 15 shows the plot of first-order and second-order Fenton reaction.

3.4. Thermodynamic of Fenton reaction

Thermodynamic parameters including Gibbs free energy change (Δ*G*°), standard enthalpy change (Δ*H*°) and standard entropy change (Δ*S*°) are the parameters to better understand the temperature effect on degradation of DB dye was studied. Gibbs free energy by using equilibrium constant K_C is calculated:

$$\Delta G° = -RT\mathrm{Ln}K_C \quad (12)$$

K_C values calculated from the following formula:

$$K_C = C_{(Ae)}/C_{(Se)} \quad (13)$$

where $C_{(Ae)}$ is amount of degradation dye at equilibrium and $C_{(Se)}$ equilibrium concentration of dye at the solution.

Table 1
Thermodynamic parameters for Fenton oxidation of DB

T (K)	K_C	Δ*G*° (kJ mol^{-1})	Δ*S*° (J mol^{-1} K^{-1})	Δ*H*° (kJ mol^{-1})
298	8.70	–5.363	261.08	–7.219
308	24.14	–8.153		
318	40.06	–9.756		
328	188.3	–14.290		

Standard enthalpy change (Δ*H*°) and standard entropy change (Δ*S*°) are as van 't Hoff equation:

$$\mathrm{Ln}K_C = -\Delta H°/RT + \Delta S°/R \quad (14)$$

In this equation, *R* is the gas constant equal to the public (8.314 J mol^{-1} K^{-1}). The amount of degradation dye at equilibrium and different temperatures 25°C–55°C have been examined to obtain thermodynamic parameters for Fenton oxidation of reaction of DB. Δ*H*° and Δ*S*° were calculated the slope and intercept of van 't Hoff plots of lnK_C vs. 1/*T*. The results of thermodynamic parameters are given in Table 1. As observed in Table 1, negative value of Δ*G*° at different temperatures (25°C–55°C) shows the oxidation process is spontaneous. The Δ*H*° negative value indicates that the uptake is exothermic [48,49] (Table 1).

3.5. Stability and recycling of the catalyst

For a practical application of a heterogeneous catalytic system, it is crucial to evaluate the stability of the catalysts. The investigations on the reusability of the HAP were examined. The physically regeneration of HAP was done by calcination of HAP adsorbed DB at 200°C for 3 h. The regeneration cycles were carried out 2, 4, 6 and 8 times. The regenerated HAP was reused for the catalytic oxidation experiments. The results were shown the value of cycles respond to the catalytic capacity of the original HAP. The catalytic capacity of the HAP did not have significant decrease after four cycles. Generally, the catalytic capacity of the HAP decreases as the number of regeneration cycle increases from 4 to 8.

4. Conclusion

Nanoparticles of HAP were successfully prepared through a simple and economical precipitation method. The structure of HAP was confirmed by FTIR, XRD, SEM and TEM analyses. The activity of HAP for Fenton catalytic oxidation of DB was studied. The oxidation of DB at different conditions was investigated. The results showed the highest oxidation efficiency of DB at pH 6, hydrogen peroxide 100 mg L^{-1}, iron(II) sulfate 9.8 × 10^{-3} mg L^{-1} and HAP 500 mg L^{-1} was obtained. The catalytic degradation of DB by HA was fivefold higher than the uncatalyst HAP of Fenton oxidation. The rate of oxidation of DB dye follows second-order kinetics and rate constant 2.91 × 10^{-1} mg L^{-1} min^{-1}. The method is applied successfully and spontaneously to degrade wastewater containing reactive azo dyes.

Acknowledgment

The authors wish to express their gratitude to Islamic Azad University-Yazd branch for the support of this work.

References

[1] C. Bauer, P. Jacques, A. Kalt, Photooxidation of an azo dye induced by visible light incident on the surface of TiO_2, J. Photochem. Photobiol., A, 140 (2001) 87–92.
[2] S. Tunç, T. Gürkan, O. Duman, On-line spectrophotometric method for the determination of optimum operation parameters on the decolorization of Acid Red 66 and Direct Blue 71 from aqueous solution by Fenton process, Chem. Eng. J., 181–182 (2012) 431–442.
[3] S. Hashemian, K. Salari, Z. Atashi, Preparation of activated carbon from agricultural wastes (almond shell and orange peel) for adsorption of 2-pic from aqueous solution, J. Ind. Eng. Chem., 20 (2013) 1892–1900.
[4] S. Hashemian, M. Mirshamsi, Kinetic and thermodynamic of adsorption of 2-picoline by sawdust from aqueous solution, J. Ind. Eng. Chem., 18 (2012) 2010–2015.
[5] S. Hashemian, M. Salimi, Nano composite a potential low cost adsorbent for removal of cyanine, Chem. Eng. J., 188 (2012) 57–63.
[6] M.R. Gadekar, M. Mansoor Ahammed, Coagulation/flocculation process for dye removal using water treatment residuals: modelling through artificial neural networks, Desal. Wat. Treat., 57 (2016) 26392–26400.
[7] V. Lavtižar, C.A. Van Gestel, D. Dolenc, P. Trebše, Chemical and photochemical degradation of chlorantraniliprole and characterization of its transformation products, Chemosphere, 95 (2014) 408–414.
[8] K.Y. Foo, B.H. Hameed, An overview of dye removal via activated carbon adsorption process, Desal. Wat. Treat., 19 (2010) 255–274.
[9] O. Duman, S. Tunç, T. Gürkan Polat, Adsorptive removal of triarylmethane dye (Basic Red 9) from aqueous solution by sepiolite as effective and low-cost adsorbent, Microporous. Mesoporous. Mater., 210 (2015) 176–184.
[10] O. Duman, S. Tunç, T. Gürkan Polat, Determination of adsorptive properties of expanded vermiculite for the removal of C. I. Basic Red 9 from aqueous solution: kinetic, isotherm and thermodynamic studies, Appl. Clay Sci., 109–110 (2015) 22–32.
[11] O. Duman, S. Tunç, T. Gürkan Polat, B. Kancı Bozoğlan, Synthesis of magnetic oxidized multiwalled carbon nanotube-κ-carrageenan-Fe_3O_4 nanocomposite adsorbent and its application in cationic methylene blue dye adsorption, Carbohydr. Polym., 147 (2016) 79–88.
[12] O. Duman, S. Tunç, B. Kanc, B. Tülin, G. Polat, Removal of triphenylmethane and reactive azo dyes from aqueous solution by magnetic carbon nanotube-κ-carrageenan-Fe_3O_4 nanocomposite, J. Alloys Compd., 687 (2016) 370–383.
[13] E. Ayranci, O. Duman, Structural effects on the interactions of benzene and naphthalene sulfonates with activated carbon cloth during adsorption from aqueous solutions, Chem. Eng. J., 156 (2010) 70–76.
[14] O. Duman, E. Ayranci, Attachment of benzo-crown ethers onto activated carbon cloth to enhance the removal of chromium, cobalt and nickel ions from aqueous solutions by adsorption, J. Hazard. Mater., 176 (2010) 231–238.
[15] O. Duman, E. Ayranci, Adsorption characteristics of benzaldehyde, sulphanilic acid, and p-phenolsulfonate from water, acid, or base solutions onto activated carbon cloth, Separ. Sci. Technol., 41 (2006) 3673–3692.
[16] E. Ayranci, O. Duman, In-situ UV-visible spectroscopic study on the adsorption of some dyes onto activated carbon cloth, Separ. Sci. Technol., 44 (2009) 3735–3752.
[17] O. Duman, E. Ayranci, Adsorptive removal of cationic surfactants from aqueous solutions onto high-area activated carbon cloth monitored by in situ UV spectroscopy, J. Hazard. Mater., 174 (2010) 359–367.
[18] S. Tunç, O. Duman, T. Gürkan, Monitoring the decolorization of acid orange 8 and acid red 44 from aqueous solution using Fenton's reagents by online spectrophotometric method: effect of operation parameters and kinetic study, Ind. Eng. Chem. Res., 52 (2013) 1414–1425.
[19] S.F. Kang, C.H. Liao, M.C. Chen, Pre-oxidation and coagulation of textile wastewater by the Fenton process, Chemosphere, 46 (2002) 923–928.
[20] V. Kavitha, K. Palanivelu, Destruction of cresols by Fenton oxidation process, Water Res., 39 (2005) 3062–3072.
[21] N. Ertugay, F. Nuran Acar, Removal of COD and color from Direct Blue 71 azo dye wastewater by Fenton's oxidation: kinetic study, Arab. J. Chem., 2 (2013) S1158–S1163.
[22] J.M. Herrmann, Heterogeneous photocatalysis: state of the art and present applications, Top Catal., 35 (2005) 49–65.
[23] G.K. Pradhan, K.M. Parida, Fabrication of iron-cerium mixed oxide: an efficient photocatalyst for dye degradation, Int. J. Eng. Sci. Technol., 2 (2010) 53–65.
[24] M. Takeuchi, S. Sakai, A. Ebrahimi, M. Matsuoka, M. Anpo, Application of highly functional Ti-oxide-based photocatalysts in clean technologies, Top. Catal., 52 (2009) 1651.
[25] J.D. Laat, H. Gallard, Catalytic decomposition of hydrogen peroxide by Fe (III) in homogeneous aqueous solution: mechanism and kinetic modeling, Environ. Sci. Technol., 33 (1999) 2726–2732.
[26] S.S. Lin, M.D. Gurol, Catalytic decomposition of hydrogen peroxide on iron oxide: kinetics, mechanisms, and implications, Environ. Sci. Technol., 32 (1998)1417–1423.
[27] J. Marugán, M.J. López-Muñoz, R. van Grieken, J. Aguado, Photocatalytic decolorization and mineralization of dyes with nano crystalline TiO_2/SiO_2 materials, Ind. Eng. Chem. Res., 46 (2007) 7605–7610.
[28] S.A. Elfeky, A.S.A. Al-Sherbini, Photocatalytic decomposition of trypan blue over nanocomposite thin films, Kinet. Catal., 52 (2011) 391–396.
[29] D. Zhang, H. Zhao, X. Zhao, Y. Liu, X. Li, Application of hydroxyapatite as catalyst and catalyst carrier, Prog. Chem., 23 (2011) 687–694.
[30] Z. Yaakob, L. Hakim, M.N. Satheesh Kumar, M. Ismail, W.R.W. Daud, Hydroxyapatite supported nickel catalyst for hydrogen production, Am. J. Sci. Ind. Res., 1 (2010) 122–126.
[31] A. Venugopal, M.S. Scurrell, Hydroxyapatite as a novel support for gold and ruthenium catalysts: behaviors in the water gas shift reaction, Appl. Catal., A, 245 (2003) 137–147.
[32] N. Phonthammachai, J. Kim, T.J. White, Synthesis and performance of a photo catalytic titania-hydroxyapatite composite, J. Mater. Res., 9 (2008) 2398–2405.
[33] T. Hara, K. Mori, M. Oshiba, T. Mizugaki, K. Ebitani, K. Kaneda, Highly efficient dehalogenation using hydroxyapatite supported palladium nanocluster catalyst with molecular hydrogen, Green Chem., 6 (2004) 507–509.
[34] Z.P. Yang, C.J. Zhang, Adsorption and photocatalytic degradation of bilirubin on hydroxyapatite coatings with nanostructural surface, J. Mol. Catal. A: Chem., 302 (2009) 107–111.
[35] M.P. Reddy, A. Venugopal, M. Subrahmanyam, Hydroxyapatite photocatalytic degradation of calmagite (an azo dye) in aqueous suspension, Appl. Catal. B: Environ., 69 (2007) 164–170.
[36] Z.P. Yang, X.U. Gong, C.J. Zhang, Recyclable Fe_3O_4/hydroxyapatite composite nanoparticles for photocatalytic applications, Chem. Eng. J., 165 (2010) 117–121.
[37] S. Hamzah, M.F.M. Salleh, Hydroxyapatite/chitosan biocomposite for remazol blue dyes removal, Appl. Mech. Mater., 695 (2014) 106–109.
[38] M. Stylidi, D.I. Kondarides, X.E. Verykios, Pathways of solar light induced photo catalytic degradation of azo dyes in aqueous TiO_2 suspensions, Appl. Catal. B: Environ., 40 (2003) 271–286.
[39] H. Nishikawa, K. Omamiuda, Photocatalytic activity of hydroxyapatite for methyl mercaptane, J. Mol. Catal. A: Chem., 179 (2002) 193–200.
[40] C. Rey, J. Lian, M. Grynpas, F. Shapiro, L. Zulkerg, M.J. Glimcher, Non-apatitic environments in bone mineral: FTIR

detection, biological properties and changes in several disease states, Connect. Tissue Res., 21 (1989) 267–273.
[41] N. Barka, S. Qourzal, A. Assabbane, A. Nounah, Y. Ait-Ichou, Removal of reactive yellow 84 from aqueous solutions by adsorption onto hydroxyapatite, J. Saudi Chem. Soc., 15 (2011) 263–267.
[42] C. Bouasla, M. El-Hadi Samar, F. Ismail, Degradation of methyl violet 6B dye by the Fenton process, Desalination, 254 (2010) 35–41.
[43] F. Fu, Q. Wang, B. Tang, Effective degradation of C.I. Acid Red 73 by advanced Fenton process, J. Hazard. Mater., 174 (2010) 17–22.
[44] M.S. Lucas, J.A. Peres, Decolorization of the azo dye reactive black 5 by Fenton and photo-Fenton oxidation, Dyes Pigm., 71 (2006) 236–244.
[45] F. Emami, A.R. Tehrani-Bagha, K.F. Gharanjig, M. Menger, Kinetic study of the factors controlling Fenton-promoted destruction of a non-biodegradable dye, Desalination, 257 (2010) 124–128.
[46] S.P. Sun, C.J. Li, J.H. Sun, S.H. Shi, M.H. Fan, Q. Zhou, Decolorization of an azo dye Orange G in aqueous solution by Fenton oxidation process: effect of system parameters and kinetic study, J. Hazard. Mater., 161 (2009) 1052–1057.
[47] G.E.A. Mahmoud, L.F.M. Ismail, Factors affecting the kinetic parameters related to the degradation of direct yellow 50 by Fenton and photo-Fenton processes, J. Basic Appl. Chem., 1 (2011) 70–79.
[48] S. Hashemian, Fenton-like oxidation of malachite green solutions: kinetic and thermodynamic study, J. Chem., 2013 (2013) 1–7, Article ID 809318. Available at: http://dx.doi.org/10.1155/2013/809318.
[49] L. Nunez, J.A. Garcia-Hortal, F. Torrades, Study of kinetic parameters related to the decolourization and mineralization of reactive dyes from textile dyeing using Fenton and photo-Fenton processes, Dyes Pigm., 75 (2007) 647–652.